A two-step multiaxial racetrack filter algorithm for non-proportional load histories

Marco Antonio Meggiolaro, Jaime Tupiassú Pinho de Castro
Pontifical Catholic University of Rio de Janeiro, PUC-Rio, R. Marquês de São Vicente 225, Rio de Janeiro, 22451-900, Brazil
meggi@puc-rio.br, jtcastro@puc-rio.br

Hao Wu
School of Aerospace Engineering and Applied Mechanics Tongji University, Siping Road 1239, 200092, Shanghai, P.R.China
wuhao@tongji.edu.cn

ABSTRACT. The recently proposed multiaxial racetrack filter (MRF) is able to deal with general non-proportional multiaxial load histories. While only requiring a single user-defined scalar filter amplitude, the MRF is able to synchronously eliminate non-damaging events from any noisy multiaxial load history without changing the overall shape of its original path, a necessary condition to avoid introducing errors in fatigue damage assessments. The MRF procedures are optimized here by the introduction of a pre-processing "partitioning" step on the load history data, which selects candidates for the reversal points in a robust partitioning process, highly increasing the filter efficiency and decreasing its computational time. The improved MRF is evaluated through the fatigue analyses of over-sampled tension-torsion data measured in 316L stainless steel tubular specimens under non-proportional load paths.

KEYWORDS. Multiaxial racetrack filter (MRF); Partitioning operation; Multiaxial variable amplitude loading; Amplitude filter.

Citation: Meggiolaro, M.A., Castro, J.T.P., Wu, H., A two-step multiaxial racetrack filter algorithm for non-proportional load histories, Frattura ed Integrità Strutturale, 41 (2017) 1-7.

Received: 28.02.2017
Accepted: 15.04.2017
Published: 01.07.2017

INTRODUCTION

Fatigue load histories measured under actual field conditions usually are noisy, over-sampled, and contain too many non-damaging low-amplitude events that can largely increase the subsequent fatigue damage calculation burden. This problem has long been recognized and properly dealt with in traditional uniaxial analyses, but it is still much more important for multiaxial fatigue damage calculations, which can even become impractical if not properly filtered to remove from the data non-damaging events before performing such complex calculations, in particular under non-proportional (NP) loading conditions, so common in practical applications.

Consequently, a most important practical issue in multiaxial fatigue analyses is how to reduce a large amount of redundant multiaxial data to a manageable size to decrease their intrinsically high computational cost, while maintaining all the essential features of the load history that contribute to plasticity memory effects. Needless to say, this is an unavoidable step to not underestimate fatigue damage, an inadmissible feature in practical applications.

Uniaxial amplitude filters can be directly implemented in the cycle counting algorithm, usually based on the rainflow method [1-4]. But the original rainflow procedure can only be started after the entire load history is known, increasing even more the computational cost as well as computer memory requirements, which can be quite significant for very long histories. Computational cost can be dramatically reduced with "real-time" rainflow algorithms, such as the pioneer Martin–Topper–Sinclair's 1971 method [5], which essentially reproduces in real time the uniaxial rainflow algorithm as the load events are provided or measured. The original racetrack filter, proposed by Fuchs et al. in 1973 [6], can sequentially filter small amplitudes, but it is limited to uniaxial histories.

Simplistic amplitude filters based on the uniaxial racetrack are not recommended in multiaxial analyses, because the path between two load reversals is needed to evaluate the path-equivalent stress or strain amplitude associated with each rainflow count, e.g. using a convex-enclosure method [7, 8]. Moreover, the reversal points obtained from a multiaxial rainflow algorithm might not occur at the reversal of one of the stress or strain components [9].

In this work, a multiaxial version of the racetrack filter proposed by the authors in [10-13] is reviewed and optimized. While only requiring a single user-defined scalar filter amplitude, it is able to synchronously filter complex loading histories while preserving all key features of the loading path. The filtering process is optimized through the introduction of a pre-processing "partitioning" operation on the load history data, highly increasing its efficiency. Over-sampled experimental data from tension-torsion experiments in 316L stainless steel tubular specimens under NP load paths are used to verify the efficiency and robustness of the proposed method.

THE MULTIAXIAL RACETRACK FILTER (MRF)

In the multiaxial racetrack filter (MRF) algorithm originally proposed in [10], the load history path must first be represented in an appropriate stress or strain space. Several spaces were proposed in [11], some of them separating the stresses or strains in their deviatoric and hydrostatic components, to allow for a filtering metric based on Mises equivalent values or even damage parameters. Fig. 1 shows an example of a tension-torsion loading following an elliptical stress path, represented in a normal vs. effective shear stress space $\sigma_x \times \tau_{xy}\sqrt{3}$ through a series of 238 over-sampled points (for each periodic cycle), represented as "×" marks. However, spaces with higher dimensions would be necessary for general 6D multiaxial load histories. Several of these points could be filtered out without compromising the subsequent multiaxial fatigue life calculations.

This amplitude-filtering process is a most desirable step in practical applications, to eliminate unavoidable measurement noise and redundant over-sampled data, as well as small amplitudes that do not cause fatigue damage [12]. But it is important to avoid filtering out important counting points from multiaxial rainflow algorithms, or significant history paths that can affect the calculation of a path-equivalent stress or strain, since all stress or strain components contribute altogether for the reversals that can be eliminated.

The MRF requires a user-defined scalar filter amplitude r, which is graphically represented in Fig. 1 as the radius of the small dashed circle centered at point 1. In this example, r = 80MPa was chosen as the amplitude, which in the $\sigma_x \times \tau_{xy}\sqrt{3}$ space has a clear physical meaning: r is the Mises distance between two stress states, due to the adopted $\sqrt{3}$ scaling factor used in the shear component. The MRF algorithm, thoroughly described in [10-13], was able to reduce the 238 over-sampled measurements to only 8, guaranteeing that no filtered-out data lies beyond r = 80MPa of the resulting polygonal path 1-2-3-4-5-6-7-8-1.

This filtering process results in a dramatic decrease of the computational time needed for further multiaxial fatigue life calculations, especially considering that the original 238 points were from a single elliptical path. More refined outputs can be achieved simply by reducing the user-defined value of the (combined) amplitude filter r. For instance, in the above example, r = 5MPa would better describe the elliptical shape of the original stress path, but it would need 31 points instead of 8 to represent it; still, 31 is much better than the original 238 points per cycle. The filter amplitude r can also be varied as a function of the instantaneous normal stresses, to better consider mean and peak-stress effects, as discussed in [12]. Moreover, the MRF also works with non-periodic load histories, using the same algorithm.

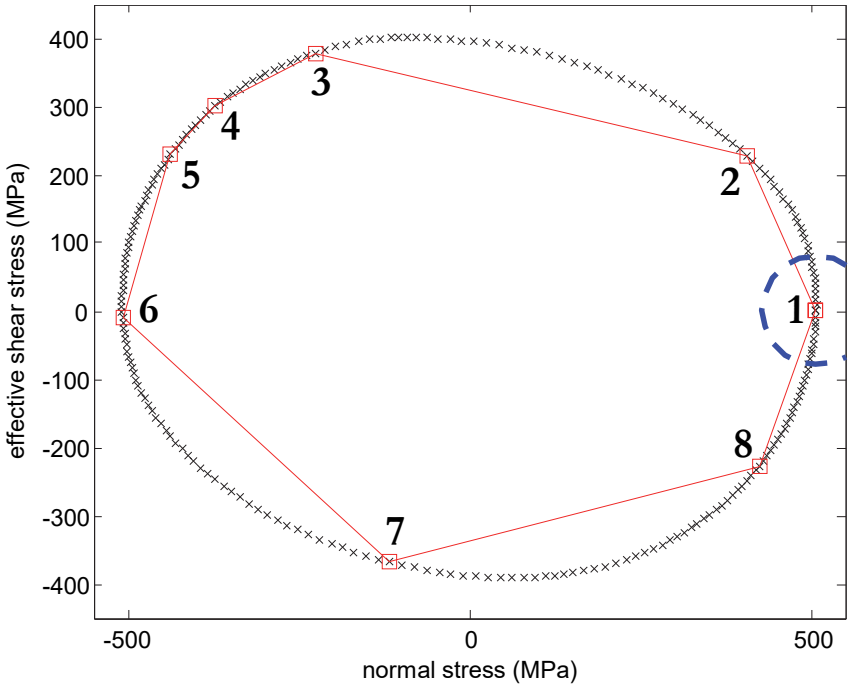

Figure 1: Application of the MRF on a tension-torsion $\sigma_x \times \tau_{xy}\sqrt{3}$ history, adopting a filter amplitude r = 80MPa.

It is important to note that the MRF does not filter out load reversals, which can be interpreted as sudden changes in path direction of more than 90 degrees. This is a major advantage over simplistic algorithms such as the "Peaks Procedure" [14], which filters out all points (events) whose components are not peaks or valleys. This non-conservative procedure potentially eliminates important load points that could have the highest Mises stresses or strains of the load history, even though each individual load component was not maximized. Moreover, the "Peaks Procedure" stores each and every event that constitutes a peak or valley from any single component, which for (unavoidably noisy) real measurements could result in no events at all being filtered out, even if the noise had very low amplitudes.

Despite its efficiency and robustness, the MRF can still be optimized to better describe the original path using the same number of sampling points. For instance, in Fig. 1 it can be seen that the segment 4-5 faithfully describes the original sampled points, however the segments 6-7 and 7-8 do not reproduce well the originally curved path. One way to improve this issue is to use a smaller filter amplitude, lower than the adopted r = 80MPa, however at a cost of filtering out fewer points, requiring more than 8 to represent the load path in this case. A more efficient way is proposed next, where a pre-processing "partitioning" operation is performed on the original sampled points, resulting in a better description of the path with fewer data points.

MRF Optimization through Partitioning

Before applying the MRF algorithm, it is here proposed to perform an improved pre-processing "partitioning" operation on the multiaxial load history data, described as follows. The first step involves choosing the first sample point of the multiaxial load history, tagged with the number 1. For periodic histories, point 1 can be any point from the cyclic load path, see Fig. 2(a).

Then, find the sampled point most distant to 1, labeling it as 2, creating two partitions of the original sample points, defined by the paths {1→2} and {2→1}. In the considered tension-torsion example in the $\sigma_x \times \tau_{xy}\sqrt{3}$ space, point 2 results in the one with the highest relative Mises stress range with respect to point 1. If more than one point has the same maximum distance from 1, then choose any one of them to become point 2, ignoring the others.

Note however that, for non-periodic load histories, points 1 and 2 should be simply defined as the first and last ones from the entire history, respectively.

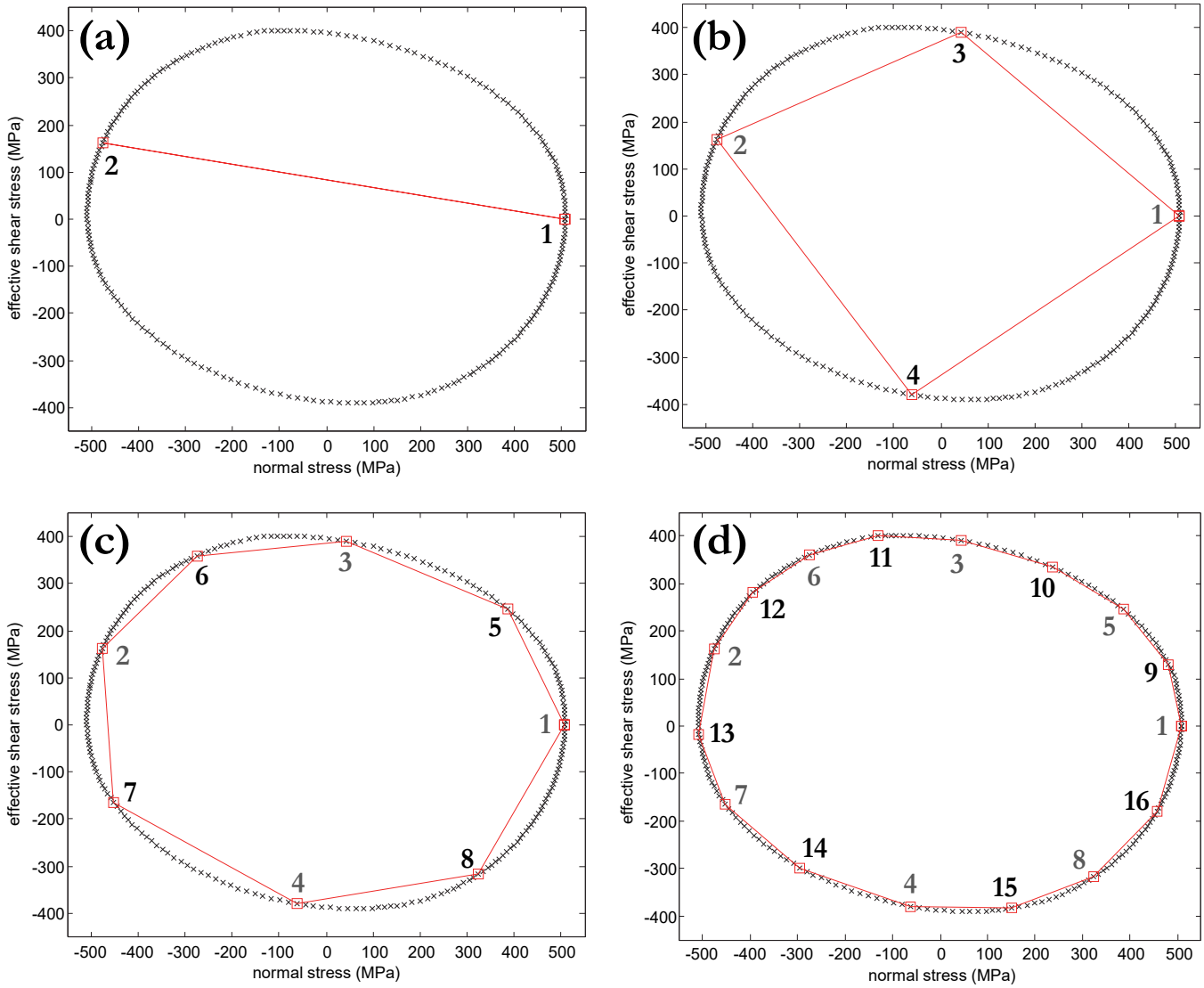

Figure 2: Improved partitioning operation on tension-torsion data, showing: (a) joining the previously defined points 1 and 2 of the load history with a straight line; (b) finding the load points 3 and 4 most distant from this line, creating two partitions; (c) finding the points most distant to each segment to subdivide it into additional segments; and (d) continuing the process until reaching the chosen filter amplitude value.

The next step of the pre-processing involves joining points 1 and 2 with a straight line, and then finding the load points 3 and 4 most distant from it. Note that point 3 lies in the 1→2 path whereas point 4 lies in the 2→1, as shown in Fig. 2(b). Since this maximum distance is higher than the chosen filter amplitude r, create further partitions {1→3}, {3→2}, {2→4} and {4→1} of the original path, see Fig. 2(b).

Next, look for the load point in the {1→3} partition that is most distant from the straight line joining 1 and 3; if this maximum distance is higher than r, then create additional two partitions {1→5} and {5→3} from {1→3}, see Fig. 2(c). Analogously, look for the load point in the {3→2} partition that is most distant from the straight line joining 3 and 2; if this maximum distance is higher than r, then create two partitions {3→6} and {6→2} from {3→2}. The process continues for the remaining partitions, as long as the associated maximum distance is still higher than r.

The pre-processing process continues for all created partitions, ending only when all such maximum distances are not higher than the chosen filter amplitude r. Consequently, each of the resulting partitions is such that all points it contains are within a distance r of the straight line joining its extremes. Note that the remaining sample points that were not labeled are not yet eliminated, because they could contain load reversions that are not detected in this pre-processing step, as discussed later.

In the studied tension-torsion example, this partitioning results in the 8 points from Fig. 2(c) for r = 80MPa. Note how the resulting polygonal path better represents the original history than the one from Fig. 1, where no pre-processing had been performed, using the same number of points. Fig. 2(d) shows the partitioning results if the filter amplitude is refined adopting r = 5MPa, resulting in 16 points per cycle, but with a better description of the load path.

After (and only after) the pre-processing partitioning ends, the MRF is individually applied to each partition, with a filter surface translation direction [10-12] defined from the extremes of each partition. For instance, for r = 80MPa, the partitioning output shown in Fig. 2(c) would require the application of the MRF on the points in the {1→5} path, starting from 1 and with a filter surface translation direction defined by the segment 1→5; then apply the MRF again in the {5→3} path, starting from 5 and in the 5→3 direction; and so on, until processing the segment {8→1}. In this particular example, all non-labelled sample points ended up filtered out by the MRF, but this might not be the case in more complex paths, as exemplified below. As a result, the output of the MRF will consist of all load points (from all partitions) that did not suffer static or dynamic filtering. This combination of partitioning followed by the MRF is very efficient, resulting in quasi-optimal filtered histories for a given r, without the need to arbitrarily define or optimize the hyper-sphere translation directions [10-12] in higher-dimensional cases.

Fig. 3 shows a more complex NP tension-torsion stress path that needs both partitioning and MRF steps to properly filter its 488 sample points (per cycle) without losing significant load reversions. Point 1 is arbitrarily chosen as the initial one in the tension-torsion cycle, and a filter amplitude of r = 80MPa is considered (graphically represented as the radius of the dashed circle around point 1). The pre-processing step then finds point 2 as the most distant from 1. Points 3 and 4 are then the ones most distant from the 1→2 straight line, both with distances greater than r = 80MPa. Since all points in the {1→3} path are within r = 80MPa of the straight segment 1→3, no further points are selected in this portion. The same applies for the {3→2}, {2→4} and {4→1} portions of the load path, ending the pre-processing step with only 4 identified points, marked with squares in Fig. 3. The MRF is then individually applied to each of these portions, using the same filter amplitude r = 80MPa, to be able to identify the important load reversal points 5, 6, 7, 8, 9 and 10, marked with triangles in Fig. 3. Note that a few load reversal points are purposely not identified, such as the ones in the {4→1} path, because their associated oscillation amplitudes are smaller than the chosen r = 80MPa, a desirable feature that the simplistic "Peaks Procedure" [14] would not be able to reproduce.

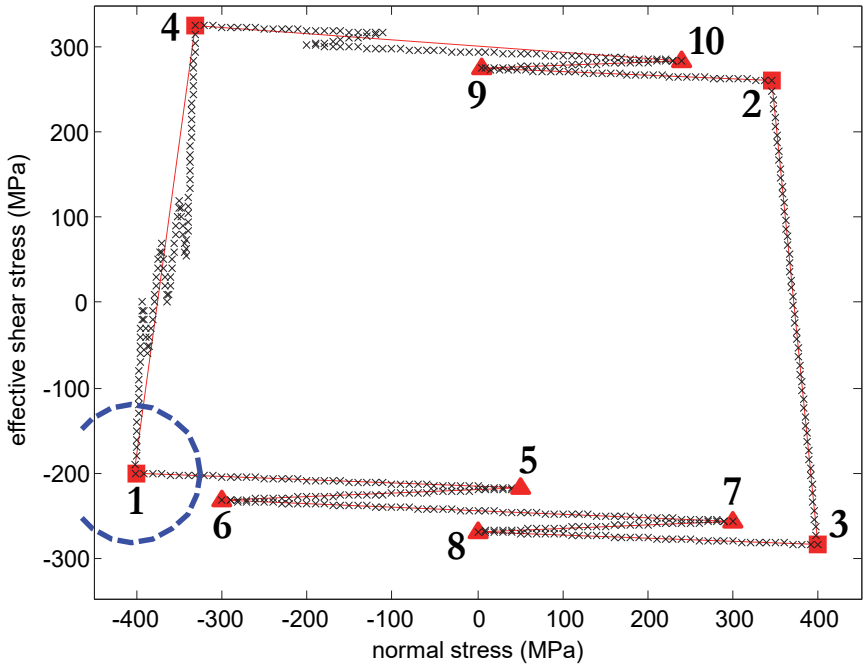

Figure 3: Tension-torsion load path with 488 sample points per cycle, where the partitioning operation identifies points 1 through 4, followed by the application of the MRF in each partition to identify points 5 through 10, adopting a filter amplitude r = 80MPa.

Experimental Verification

To verify the efficiency of the optimized MRF, tension-torsion experiments are performed on annealed tubular 316L stainless steel specimens in an MTS 809.25 multiaxial testing machine, shown in Fig. 4(a). A relatively thin wall of 2mm is used for the tubular specimens, to avoid having to deal with stress gradient effects across its thickness. Engineering stresses and strains are calculated from load/torque cell measurements and from an MTS 632.68 axial/torsional extensometer, and then converted to true stresses and strains [13]. The cyclic properties of this 316L steel are obtained from uniaxial tests, resulting in fitted Ramberg-Osgood uniaxial cyclic hardening coefficient 874MPa and exponent 0.123, with Young's modulus 193GPa, Poisson ratio 0.3, and shear modulus 74GPa.

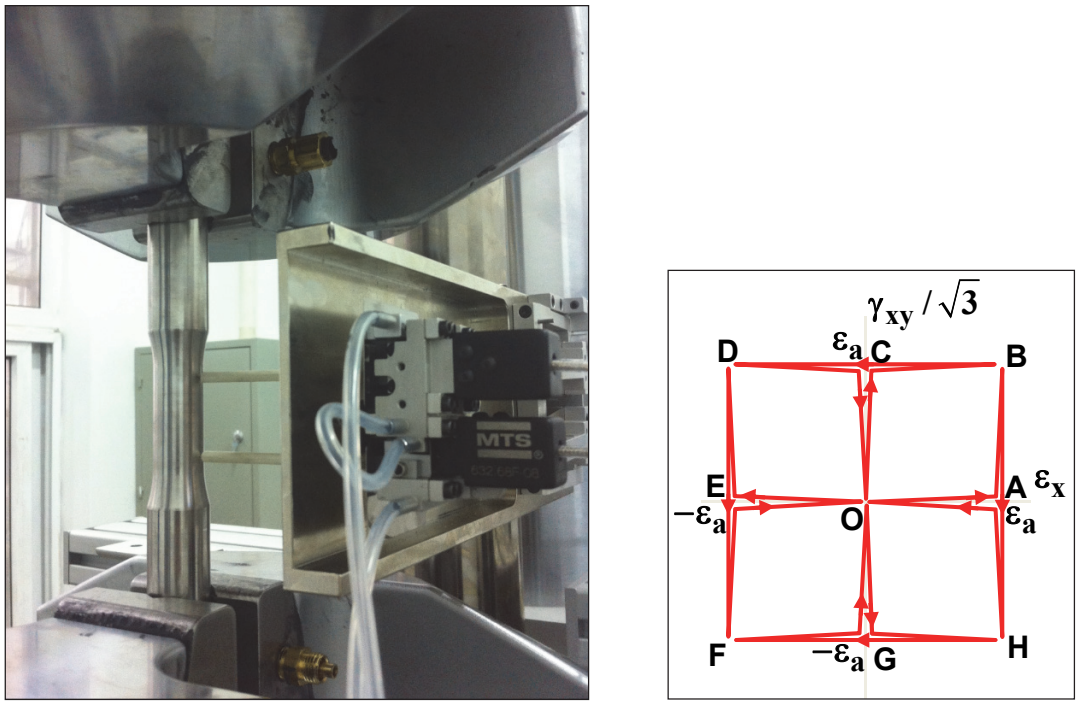

(a) (b)

Figure 4: (a) Tension-torsion testing machine and extensometer mounted on a tubular specimen; (b) applied $\varepsilon_x \times \gamma_{xy}/\sqrt{3}$ strain paths.

The tests consist of strain-controlled $\varepsilon_x \times \gamma_{xy}/\sqrt{3}$ tension-torsion cycles applied to the tubular specimens, following the very challenging cyclic path sequence OABHAOCBDCOEDFEOGHFGO, see Fig. 4(b). Fig. 5 shows the resulting experimentally measured stabilized $\sigma \times \tau\sqrt{3}$ stress path (samples with × markers), as well as the optimized MRF output including the proposed pre-processing step (square markers) for a filter amplitude r = 15MPa. The measured $\sigma \times \tau\sqrt{3}$ stress paths are reduced from 1227 data points per cycle to only 52, showing a very good agreement in both ranges and shape. Notice that, despite being highly filtered, the optimized MRF outputs can almost exactly describe the original multiaxial load history, capturing not only all reversal points but also the load path shape, which is a most important feature for path-equivalent range calculations used in fatigue damage assessments.

Conclusions

In this work, an optimized version of the multiaxial racetrack filter (MRF) was proposed, applicable to general non-proportional multiaxial histories. The MRF preserves load order, allowing the synchronous filtering of stress and strain histories, without filtering out important multiaxial load reversal points. The optimized version is based on a pre-processing step that selects candidates for the reversal points, in a robust partitioning process. The filter efficiency was validated from tension-torsion experiments following complex non-proportional histories, without losing information on significant reversals, ranges or load path shapes.

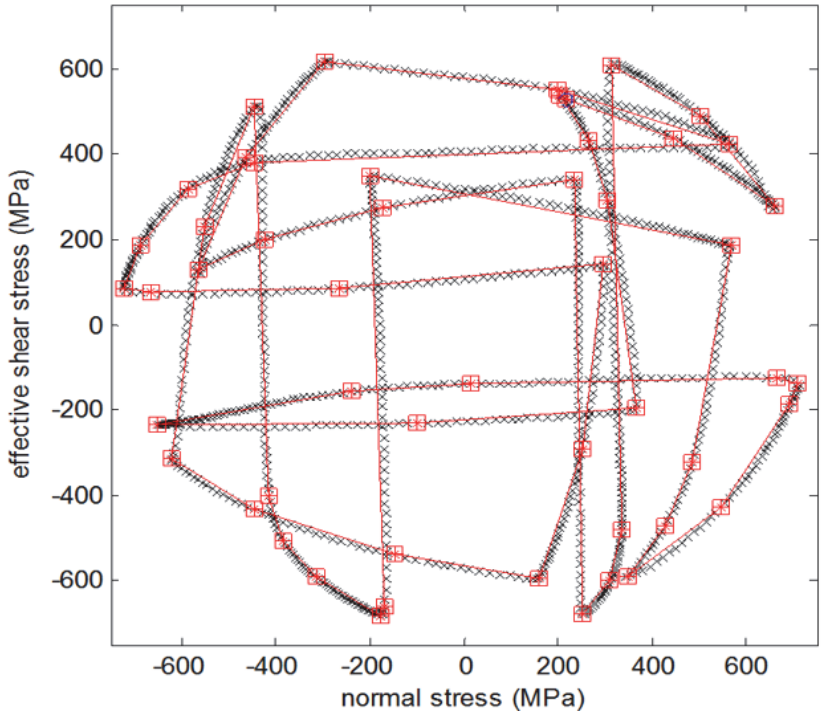

Figure 5: Experimentally measured data points (× markers) and the optimized MRF output (square markers) including the pre-processing partitioning with r = 15MPa.

REFERENCES

[1] Anthes, R.J., Modified rainflow counting keeping the load sequence, Int J Fatigue, 19 (1997) 529-535.
[2] ASTM E 1049. Standard practices for cycle counting in fatigue analysis. ASTM International.
[3] Downing, S.D., Socie, D.F. Simple rainflow counting algorithms. Int J Fatigue 4 (1982) 31-40.
[4] Bannantine, J.A., Socie, D.F. A variable amplitude multiaxial fatigue life prediction method, Fatigue Under Biaxial and Multiaxial Loading, ESIS publ. 10 (1991) 35-51.
[5] Martin, J.F., Topper, T.H., Sinclair, G.M. Computer Based Simulation of Cyclic Stress-Strain Behavior with Applications to Fatigue. Materials Research and Standards, MTRSA, 11 (1971) 23-28.
[6] Fuchs, H.O., Nelson, D.V., Burke, M.A., Toomay, T.L. Shortcuts in Cumulative Damage Analysis. SAE Automobile Engineering Meeting Paper 730565 (1973).
[7] Dang Van, K., Papadopoulos, I.V. High-cycle metal fatigue, Springer (1999).
[8] Freitas, M., Li, B., Santos, J.L.T. Multiaxial fatigue and deformation: testing and prediction. ASTM STP 1387 (2000).
[9] Meggiolaro, M.A., Castro, J.T.P. An Improved Multiaxial Rainflow Algorithm for Non-Proportional Stress or Strain Histories - Part II: The Modified Wang-Brown Method, Int J Fatigue 42 (2012) 194-206.
[10] Meggiolaro, M.A., Castro, J.T.P., Shortcuts in multiple dimensions: the multiaxial racetrack filter, Frattura e Integrità Strutturale 33 (2015), 368-375. DOI 10.3221/IGF-ESIS.33.40.
[11] Wu, H., Meggiolaro, M.A., Castro, J.T.P. Validation of the Multiaxial Racetrack Amplitude Filter, Int J Fatigue, 87 (2016), 167-179. DOI 10.1016/j.ijfatigue.2016.01.016
[12] Meggiolaro, M.A., Castro, J.T.P., Wu, H. Incorporation of Mean/Maximum Stress Effects in the Multiaxial Racetrack Filter, Frattura e Integrità Strutturale, 38 (2016), 67-75. DOI 10.3221/IGF-ESIS.38.09
[13] Castro, J.T.P., Meggiolaro, M.A. Fatigue Design Techniques, volume 2: Low-Cycle and Multiaxial Fatigue. Create Space 2016. ISBN 1530797047.
[14] Bannantine, J.A. A Variable Amplitude Multiaxial Fatigue Life Prediction Method. FCP Report n.151, University of Illinois at Urbana-Champaign (1989).